CrystEngComm

ROYAL SOCIETY OF CHEMISTRY

COMMUNICATION

Cite this: *CrystEngComm*, 2024, **26**, 2056

Received 7th February 2024,
Accepted 14th March 2024

DOI: 10.1039/d4ce00124a

rsc.li/crystengcomm

Using the nature of the achiral solvent to orient chiral resolution†

Joséphine de Meester,[a] Oleksii Shemchuk,[a] Laurent Collard,[a] Johan Wouters,[b] Simon Baillieux,[a] Koen Robeyns [a] and Tom Leyssens *[a]

We demonstrate the unprecedented phenomenon of solvent-oriented resolution of 1,1′-bi-2-naphtol (Binol). Using a resolution agent of a fixed handedness (*R*,*R*)-*N*,*N*′-dimethyl-1,2-diphenylethane-1,2-diamine (DADPE), we are able to resolve either the (*S*)- or (*R*)-enantiomer of Binol by a mere change of the achiral solvent.

Over 50% of marketed drug compounds contain a stereogenic unit. Whereas one enantiomer (the eutomer) shows a desired pharmacological effect, the other (the distomer) potentially has no, a similar, or in worst cases an adverse effect. For these latter cases, the drug can only be marketed as an enantiopure compound.[1–5] The most prominent approach to enantiopure drugs still involves the formation of a racemic mixture by non-asymmetric synthesis. The eutomer can then be resolved using a chiral resolution agent.[2,5–7]

Binol (1,1′-bi-2-naphtol) is such a highly versatile agent being used both in resolution,[8,9] as well as asymmetric reactions.[8,10–12] Accessing enantiopure Binol has substantial economic and scientific interest.[13–15] In 1993, Hirata *et al.* resolved Binol by cocrystallization with enantiopure *N*,*N*′-dimethyl-1,2-diphenylethane-1,2-diamine (DADPE).[8] They suspected the existence of a (*R*)-Binol-(*R*,*R*)-DADPE cocrystal phase ((*R*)-(*R*,*R*)) (Scheme 1). In parallel, Gawroński *et al.*[12] resolved the crystalline structure of the diastereomeric counter-pair (*S*)-Binol-(*R*,*R*)-DADPE ((*S*)-(*R*,*R*)), which was seemingly the most accessible of the two diastereomers (Scheme 1).

This apparent contradiction, incited us to explore this system in detail. Astonishingly, we found that either of the enantiomers of (*rac*)-Binol can be resolved using (*R*,*R*)-DADPE by merely changing the nature of the solvent (Fig. 1). This surprising feature originates from the fact that the (*S*)-(*R*,*R*) cocrystal is more stable compared to the (*R*)-(*R*,*R*) diastereomer, leading to resolution of (*S*)-Binol in all tested solvents, except benzene. Using the latter, a stable (*R*)-(*R*,*R*)-benzene cocrystal–solvate forms (Scheme 1). As this solvate is even more stable than the (*S*)-(*R*,*R*) cocrystal, (*R*)-Binol can be resolved when using benzene as a solvent (Fig. 1). To the best of our knowledge, we are the first to highlight how the nature of an achiral solvent can be used to direct the outcome of a chiral resolution process.

Our initial investigation of this system, started by performing congruency tests both for the (*S*)-(*R*,*R*) and (*R*)-(*R*,*R*) systems in various solvents (Table S2†). At 20 °C, the (*S*)-Binol-(*R*,*R*)-DADPE cocrystal behaves congruently in all tested solvents, with the cocrystal phase being identical to that reported previously (CCDC ref code: DICVUH[12]) (Fig. S4†). Surprisingly, the combination of (*R*)-Binol and (*R*,*R*)-DADPE resulted in two distinct phases (Fig. S5 and S6†). Identical patterns were obtained in MeOH, EtOH, EtOAc, DCM, toluene, and IPA, matching the simulated pattern of the (*R*)-

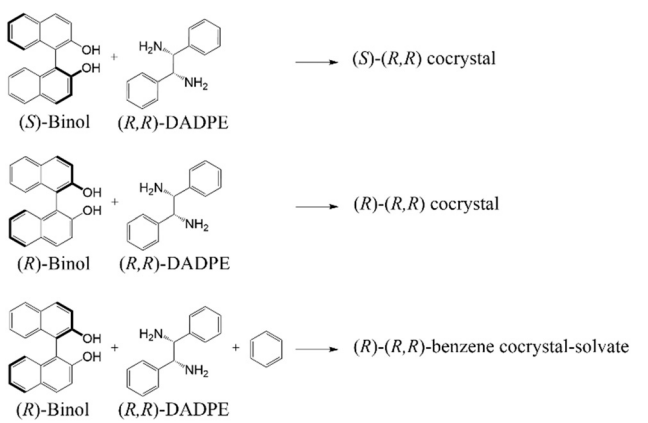

Scheme 1 (*R*)-Binol and (*S*)-Binol cocrystallize with (*R*,*R*)-DADPE, leading to a (1 : 1) diastereomeric cocrystal pair. (*R*)-Binol also forms an enantiospecific cocrystal–solvate with (*R*,*R*)-DADPE and benzene.

[a] *Institute of Condensed Matter and Nanosciences, UCLouvain, Place Louis Pasteur 1, 1348 Louvain-la-Neuve, Belgium. E-mail: tom.leyssens@uclouvain.be*
[b] *Department of Chemistry, Université de Namur, UNamur, Rue de Bruxelles 61, 5000 Namur, Belgium*

† Electronic supplementary information (ESI) available: The authors have cited additional references within the ESI.[27–32] CCDC 2295235 and 2295236. For ESI and crystallographic data in CIF or other electronic format see DOI: **https://doi.org/10.1039/d4ce00124a**

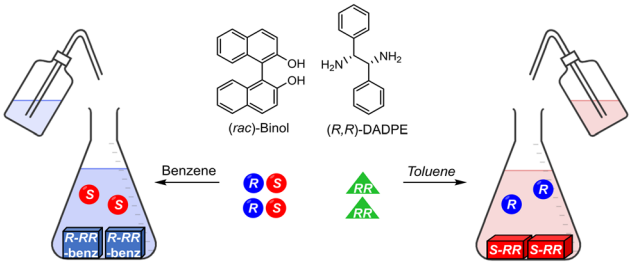

Fig. 1 A mere choice of solvent allows targeting either one of the two enantiomers of Binol using (*R*,*R*)-DADPE as resolution agent.

(*R*,*R*) cocrystal, which structure we determined (Table S1, Fig. S1 and S5†).‡ In benzene, however, a different solid form was obtained. Single crystal analysis shows this form to be a co-crystal-solvate (Table S1, Fig. 2, S2 and S6†)‡ characterized by a porous structure, with two distinct benzene sites. The first site, shows benzene located in a pocket surrounded by aromatic rings in close proximity to a crystallographic 2-fold axis (Fig. 2, in blue) while the second site shows benzene covering the surface of a channel along the 4-fold axis (Fig. 2, in green). The crystal diffracted poorly, allowing only partial localisation of the benzene solvent molecules (see ESI†).

Thermal analysis confirms the presence of distinct solvate sites.§ Gravimetric analysis (Fig. S9†) shows a first gradual mass loss occurring up to 50 °C likely corresponding to benzene loosely retained inside the channels. This loss is no longer present after having stored the sample for multiple days under ambient conditions (Fig. S10†). At 50 °C a more abrupt loss is observed, likely corresponding to remaining benzene covering the inside of the voids (green in Fig. 2). Both combined losses correspond to an 8.7% weight loss representing 0.6 equivalents of benzene. A DSC-endotherm at 50 °C (Fig. S13†) aligns with this first desolvation process, with VT-XRPD (Fig. S14–S17†) showing minor peak modifications at 55 °C characteristic of a slight change in the crystal structure. The loss of the benzene molecules located at the second site (blue in Fig. 2), is observed at 75 °C, characterized by a weight loss of 7.11%, corresponding to 0.5 equivalents of benzene. DSC shows the characteristic desolvation endotherm, with a VT-XRPD showing a transition to the non-solvated (*R*)-(*R*,*R*) cocrystal phase. The similar structural motifs of the non-solvated and solvated phases (Fig. S3†) are indicative of a true solid–solid transition during desolvation, with the non-solvated phase no longer presenting a pore-like structure and a resulting higher density (Table S1†). The non-solvated cocrystal melts at 130 °C (Fig. S12 and S13†).

To identify the potential diastereomeric (*S*)-(*R*,*R*)-benzene cocrystal–solvate a multitude of experiments were performed. Several months of work did not lead to the successful identification of such a form, allowing us to conclude the solvated system behaves enantiospecifically,[16] with the (*S*)-(*R*,*R*)-benzene never crystallizing. To our knowledge, this is the first occurrence of a solvent inducing cocrystal enantiospecificity, with the non-solvated system behaving diastereomerically.

The relative stability between the non-solvated diastereomeric (*R*)-(*R*,*R*) and (*S*)-(*R*,*R*) cocrystals was determined based on their solubility in various solvents, excluding benzene. The (*S*)-(*R*,*R*) diastereomer is the less soluble of both (Table 1), and hence thermodynamically more stable in the range of 10 °C to 60 °C (Fig. S18–S21†).[17,20] This implies that (*R*,*R*)-DADPE can be used to resolve (*S*)-Binol from a racemate using any tested solvent but benzene.

Switching to benzene, the (*R*)-(*R*,*R*)-benzene cocrystal–solvate shows lower solubility compared to the (*S*)-(*R*,*R*) cocrystal (Table 1 and Fig. S22†). This (*R*)-(*R*,*R*)-benzene cocrystal solvate is therefore thermodynamically favored in a benzene suspension.¶ Interestingly, this implies (*R*,*R*)-DADPE can once more be used, but this time to resolve (*R*)-Binol from a racemate.

While, in general, the handedness of the resolution agent needs to be changed to target the counter-enantiomer of a molecule to resolve,[17] here we show an original approach where the nature of the non-chiral solvent orients the resolution process. Using the same resolution agent, (*R*,*R*)-DADPE, (*S*)-Binol can be recovered using benzene, whereas (*R*)-Binol can be recovered using any other tested solvent.

We showcase this potential focusing on processes based on toluene and benzene. Both were chosen as they are structurally similar and furthermore toluene shows a significant solubility difference between the two diastereomeric cocrystals.

To establish the resolution processes isoplethal ternary phase-diagrams of both the (*rac*)-Binol-(*R*,*R*)-DADPE-toluene and

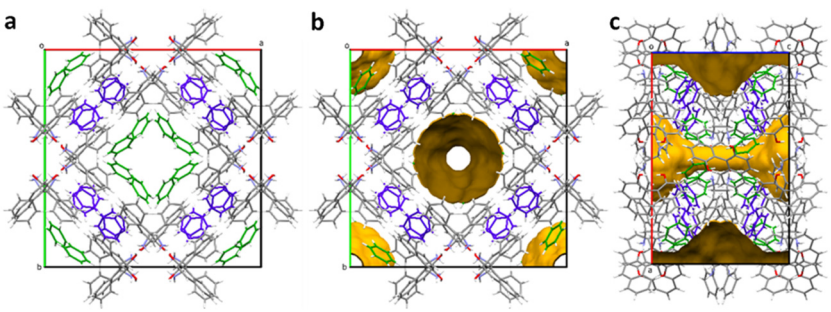

Fig. 2 Packing of the (*R*)-(*R*,*R*)-benzene cocrystal–solvate viewed along the *c*-axis (a and b) and along the *b*-axis (c). Benzene molecules occupying different sites are represented in blue (surrounded by aromatic rings) and in green (surface of the channel). Voids are shown in (b) and (c), they are represented using Mercury, with a probe radius of 1.2 Å, an approx. Grid spacing of 0.3 Å and calculated using the contact surface.

Table 1 Solubility of the solid forms in various solvents, at 20 °C. The values were taken from the solubility curves (Fig. S18–S22†)

	MeOH	EtOH	IPA	Toluene	Benzene
$C_{(R)\text{-}(R,R)}$ (mg mL^{-1})	204.44	78.40	34.10	48.29	—
$C_{(S)\text{-}(R,R)}$ (mg mL^{-1})	199.00	66.29	14.04	5.81	40.21
$C_{(R)\text{-}(R,R)\text{-benzene}}$ (mg mL^{-1})	—	—	—	—	18.15[a]

[a] The solubility of the cocrystal–solvate is expressed in mg of (*R*)-(*R*,*R*)-benzene solvate *vs.* overall amount of benzene present.

(*rac*)-Binol-(*R*,*R*)-DADPE-benzene systems were constructed. These are cross-sections of the full quaternary diagram,[3,18–20] for which the apexes are composed of (*R*)-Binol; (*S*)-Binol; (*R*,*R*)-DADPE and the solvent. For both isoplethal diagrams the overall composition in Binol (solid and solution phases combined) is always racemic. The diagrams serve to determine conditions under which resolution occurs. To construct these cross-sections a set of vials with varying composition of (*rac*)-Binol, (*R*,*R*)-DADPE, and the solvent (Tables S8 and S9†), were prepared, seeded with all possible forms, and left to equilibrate. Upon filtration, the solid phases were analyzed. Fig. 3 displays both diagrams showing the thermodynamically stable phases in suspension.

Both diagrams show similar features. Looking at the lower parts of the diagrams (lower amount of solvent), from left to right, a first zone corresponds to suspensions where (*rac*)-Binol is the only stable phase in suspension, as would be expected for overall compositions containing a large excess of (*rac*)-Binol (Fig. 3, yellow squares). As more (*R*,*R*)-DADPE is added, a zone is found, characterized by a suspension of (*rac*)-Binol combined with the most stable cocrystal (Fig. 3a: (*rac*)-Binol + (*S*)-(*R*,*R*) in red triangles; Fig. 3b: (*rac*)-Binol + (*R*)-(*R*,*R*)-benzene in red dots). Increasing the amount of (*R*,*R*)-DADPE even further, the second, less stable cocrystal also appears, leading to a zone containing three solid forms in suspension (Fig. 3a: (*rac*)-Binol + (*S*)-(*R*,*R*) + (*R*)-(*R*,*R*) in pink triangles; Fig. 3b: (*rac*)-Binol + (*R*)-(*R*,*R*)-benzene + (*S*)-(*R*,*R*) in orange dots). Still higher amounts of (*R*,*R*)-DADPE lead to a suspension of the two cocrystal phases, with this zone being larger using benzene as a solvent (Fig. 3a: (*S*)-(*R*,*R*) + (*R*)-(*R*,*R*) as a purple triangle; Fig. 3b: (*R*)-(*R*,*R*)-benzene + (*S*)-(*R*,*R*) in violet dots). Further addition of (*R*,*R*)-DADPE, then leads to the zone of interest for resolution, with only the targeted cocrystal being the stable phase in suspension (Fig. 3a: (*S*)-(*R*,*R*) in blue diamonds; Fig. 3b: (*R*)-(*R*,*R*)-benzene in pink diamonds). When the amount of (*R*,*R*)-DADPE added becomes too important, a zone is encountered where the cocrystal of interest crystallizes simultaneously with (*R*,*R*)-DADPE (Fig. 3a: (*S*)-(*R*,*R*) + (*R*,*R*)-DADPE in dark blue triangles; Fig. 3b: (*R*)-(*R*,*R*)-benzene + (*R*,*R*)-DADPE in dark blue dots). Finally, excessive amounts of (*R*,*R*)-DADPE lead to a suspension of this compound only (Fig. 3: rightmost regions of the diagrams, green squares).

For higher amounts of solvent, a similar behavior occurs going from left to right throughout the diagrams, with the difference that suspensions containing three solid forms no longer occur.

As mentioned, these diagrams allow setting conditions for the effective resolution of both enantiomers of Binol using (*R*,*R*)-DADPE as a resolution agent, using respectively toluene or benzene.

Based on these diagrams, resolution was successfully conducted on a 2-gram scale using both toluene or benzene as solvent. This led to the recovery of (*S*)- and (*R*)-Binol with respectively an ee > 97% (Fig. S24 and S25†) and ee > 99% (Fig. S26 and S27†).‖ To highlight the symmetry of the

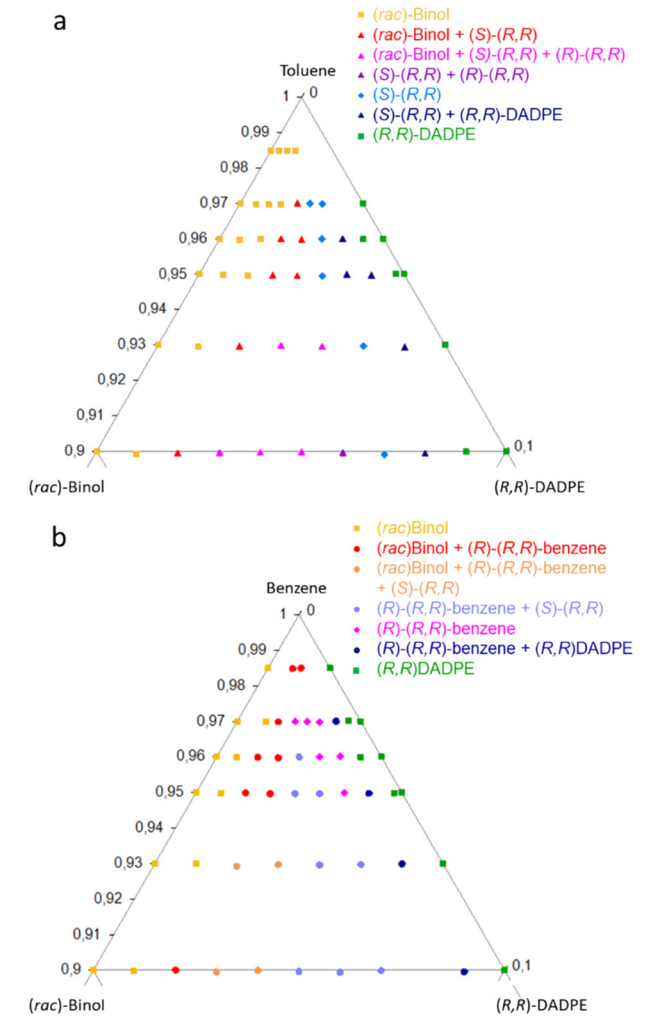

Fig. 3 Isoplethal ternary phase diagram of the system (*rac*)-Binol-(*R*,*R*)-DADPE-solvent, at 20 °C, in toluene (a) and benzene (b). Delimiting lines are not added to the diagram, as drawing these would require a more important number of experiments.

system, resolution of Binol was performed using (*S*,*S*)-DADPE in benzene, leading as expected to the recovery of the (*S*)-(*S*, *S*)-benzene cocrystal–solvate (Fig. S23†).

This contribution showcases the use of an achiral solvent to orient the outcome of a resolution process. We are the first to show how both (*R*)- and (*S*)-Binol can be resolved from a racemic mixture using (*R*,*R*)-DADPE as a resolving agent. To achieve this astonishing feature, we merely adapt the nature of the solvent, using toluene to target the (*S*)-, and benzene to target the (*R*)-enantiomer. This peculiarity finds its origin in the existence of both a diastereomeric cocrystal system, as well as an enantiospecific benzene solvate system. Guided by the thermodynamics of the system, we successfully developed an upscaled resolution leading to the recovery of (*S*)-Binol with an ee $>$ 97% using toluene and (*R*)-Binol with an ee $>$ 99% using benzene. We believe such systems will be further explored as the number of cocrystal solvates increases.[21–26]

Conflicts of interest

The authors declare no conflicts of interest.

Acknowledgements

The authors would like to thank the FNRS (PDR T.0262.20) for funding.

Notes and references

‡ Deposition numbers 2295235 (a), and 2295236 (b) contain the Supplementary Crystallographic Data for this paper.

§ Slight variations in onset temperature can occur due to different experimental setups between TGA, DSC, and VT-XRPD.

¶ The stability of a solvate depends on the temperature. Fig. S22† shows the benzene solvate to be stable up to 40 °C at least.

‖ The resolution processes presented here are conducted at 20 °C, and could be further optimized working at different temperatures.

1 L. A. Nguyen, H. He and C. Pham-Huy, *Int. J. Biomed. Sci.*, 2006, **2**(2), 85–100.
2 J. I. Putman and D. W. Armstrong, *Chirality*, 2022, **34**(10), 1338–1354.
3 M. H. Bosits, L. Bereczki, P. Bombicz, Z. Szalay, H. Pataki and Á. Demeter, *CrystEngComm*, 2023, **25**(4), 641–652.
4 I. P. Silvestri and P. J. J. Colbon, *ACS Med. Chem. Lett.*, 2021, **12**(8), 1220–1229.
5 A. Calcaterra and I. D'Acquarica, *J. Pharm. Biomed. Anal.*, 2018, **147**, 323–340.
6 Y. Teng, C. Gu, Z. Chen, H. Jiang, Y. Xiong, D. Liu and D. Xiao, *Chirality*, 2022, **34**(8), 1094–1119.
7 H. Lorenz and A. Seidel-Morgenstern, *Angew. Chem., Int. Ed.*, 2014, **53**, 1218–1250.
8 M. Kawashima and R. Hirata, *Bull. Chem. Soc. Jpn.*, 1993, **66**(7), 2002–2005.
9 E. Tayama and H. Tanaka, *Tetrahedron Lett.*, 2007, **48**(24), 4183–4185.
10 J. M. Brunel, *Chem. Rev.*, 2005, **105**(3), 857–898.
11 Y. Chen, S. Yekta and A. K. Yudin, *Chem. Rev.*, 2003, **103**(8), 3155–3212.
12 M. Ratajczak-Sitarz, A. Katrusiak, K. Gawrońska and J. Gawroński, *Tetrahedron: Asymmetry*, 2007, **18**(6), 765–773.
13 B. Love, *Curr. Org. Synth.*, 2006, **3**(2), 169–185.
14 S. Ayad, V. Posey, A. Das, J. M. Montgomery and K. Hanson, *Chem. Commun.*, 2019, **55**(9), 1263–1266.
15 N. Vu, G. M. McLeod, K. Hanson and A. E. DePrince, *J. Phys. Chem. A*, 2022, **126**(49), 9303–9312.
16 G. Springuel and T. Leyssens, *Cryst. Growth Des.*, 2012, **12**(7), 3374–3378.
17 M. Guillot, J. de Meester, S. Huynen, L. Collard, K. Robeyns, O. Riant and T. Leyssens, *Angew. Chem.*, 2020, **132**, 11303–11306.
18 F. Zhou, L. Collard, K. Robeyns, T. Leyssens and O. Shemchuk, *Chem. Commun.*, 2022, **58**, 8560–8563.
19 G. Springuel, L. Collard and T. Leyssens, *CrystEngComm*, 2013, **15**(39), 7951.
20 M. D. Charpentier, R. Venkatramanan, C. Rougeot, T. Leyssens, K. Johnston and J. H. ter Horst, *Mol. Pharmaceutics*, 2023, **20**(1), 616–629.
21 S. Aitipamula, P. S. Chow and R. B. H. Tan, *Cryst. Growth Des.*, 2010, **10**(5), 2229–2238.
22 E. Grothe, H. Meekes, E. Vlieg, J. H. ter Horst and R. de Gelder, *Cryst. Growth Des.*, 2016, **16**(6), 3237–3243.
23 A. M. Healy, Z. A. Worku, D. Kumar and A. M. Madi, *Adv. Drug Delivery Rev.*, 2017, **117**, 25–46.
24 S. P. Yelgaonkar, G. Campillo-Alvarado and L. R. MacGillivray, *J. Am. Chem. Soc.*, 2020, **142**(49), 20772–20777.
25 I. Sathisaran and S. V. Dalvi, *Cryst. Growth Des.*, 2021, **21**(4), 2076–2092.
26 T. R. Shaikh, N. Shelke and S. Tothadi, *ACS Omega*, 2023, **8**(27), 24644–24653.
27 *CrysAlisPro, Version 1.171.37.35*, Rigaku Oxford Diffraction.
28 G. M. Sheldrick, *Acta Crystallogr., Sect. A: Found. Adv.*, 2015, **71**, 3–8.
29 G. M. Sheldrick, *Acta Crystallogr., Sect. C: Struct. Chem.*, 2015, **71**, 3–8.
30 A. L. Spek, *Acta Crystallogr., Sect. D: Biol. Crystallogr.*, 2009, **65**, 148–155.
31 C. F. Macrae, I. Sovago, S. J. Cottrell, P. T. A. Galek, P. McCabe, E. Pidcock, M. Platings, G. P. Shields, J. S. Stevens, M. Towler and P. A. Wood, *J. Appl. Crystallogr.*, 2020, **53**(1), 226–235.
32 A. L. Spek, *Acta Crystallogr., Sect. C: Struct. Chem.*, 2015, **71**, 9–18.